

# Squark and gaugino hadroproduction and decays in non-minimal flavour violating supersymmetry

Björn Herrmann

Laboratoire de Physique Subatomique et de Cosmologie  
Université Joseph Fourier / CNRS-IN2P3 / INPG, 53 Avenue des Martyrs, 38026 Grenoble, France

September 11, 2007

**Abstract.** We implement non-minimal flavour violation (NMFV) in the MSSM at low scale. In this framework, we propose benchmark points for the mSUGRA scenario including non-minimal flavour violation by evaluating a number of experimental low-energy, electroweak precision and cosmological constraints. We finally discuss phenomenological aspects of our NMFV scenario and present a numerical analysis of squark and gaugino production cross sections at the LHC.

**PACS.** 12.60.Jv Supersymmetric models

## 1 Flavour violation in the MSSM

While the only source of flavour violation in the Standard Model (SM) arises through the rotation of the quark interaction eigenstates into the basis of physical mass eigenstates, in Supersymmetry (SUSY) additional flavour violation is introduced at the weak scale through renormalization group running [1]. In minimal flavour violating (MFV) scenarios, the non-diagonal entries of the squared squark mass matrices stem from the trilinear Yukawa couplings of the fermion and Higgs supermultiplets and the resulting different renormalizations of quarks and squarks. In constrained MFV (cMFV) scenarios, these flavour violating entries are neglected at the SUSY breaking and weak scale.

However, when SUSY is embedded in larger structures such as GUT theories, new sources of flavour violation arise [2], that have to be included in the squared squark mass matrices at the weak scale. As the corresponding flavour violating off-diagonal entries  $\Delta_{ij}^{qq'}$  cannot be simply deduced from the CKM-matrix alone, in NMFV is parametrized by considering them as free parameters. Denoting  $M_{Lk}^2$ ,  $M_{Rk}^2$  and  $m_k X_k$  their usual diagonal and helicity mixing entries,  $k = 1, 2, 3$  referring to the (s)quark family, the squared squark mass matrices are then given by

$$M_{\tilde{q}}^2 = \begin{pmatrix} M_{L1}^2 & \Delta_{LL}^{12} & \Delta_{LL}^{13} & m_1 X_1 & \Delta_{LR}^{12} & \Delta_{LR}^{13} \\ \Delta_{LL}^{21} & M_{L2}^2 & \Delta_{LL}^{23} & \Delta_{LR}^{21} & m_2 X_2 & \Delta_{LR}^{23} \\ \Delta_{LL}^{31} & \Delta_{LL}^{32} & M_{L3}^2 & \Delta_{LR}^{31} & \Delta_{LR}^{32} & m_3 X_3 \\ m_1 X_1^* & \Delta_{RL}^{12} & \Delta_{RL}^{13} & M_{R1}^2 & \Delta_{RR}^{12} & \Delta_{RR}^{13} \\ \Delta_{RL}^{21} & m_2 X_2^* & \Delta_{RL}^{23} & \Delta_{RR}^{21} & M_{R2}^2 & \Delta_{RR}^{23} \\ \Delta_{RL}^{31} & \Delta_{RL}^{32} & m_3 X_3^* & \Delta_{RR}^{31} & \Delta_{RR}^{32} & M_{R3}^2 \end{pmatrix}. \quad (1)$$

The scaling of the flavour violating entries  $\Delta_{ij}^{qq'}$  with the SUSY-breaking scale  $M_{\text{SUSY}}$  implies a hierarchy  $\Delta_{LL}^{qq'} \gg \Delta_{RL,LR}^{qq'} \gg \Delta_{RR}^{qq'}$  [2]. The numerically largest  $\Delta_{LL}^{qq'}$  are also related by  $SU(2)$  gauge invariance through the CKM-matrix, not allowing a large difference between them. They are usually normalized to the diagonal entries [3],

$$\Delta_{ij}^{qq'} = \lambda_{ij}^{qq'} M_{i_q} M_{j_{q'}}, \quad (2)$$

so that NMFV is governed by 24 arbitrary dimensionless parameters  $\lambda_{ij}^{qq'}$ .

The diagonalization of the mass matrices  $M_{\tilde{u}}^2$  and  $M_{\tilde{d}}^2$  requires the introduction of two additional  $6 \times 6$  matrices  $R^u$  and  $R^d$ , which relate the helicity eigenstates to the physical mass eigenstates through

$$(\tilde{u}_1, \dots, \tilde{u}_6)^T = R^u(\tilde{u}_L, \tilde{c}_L, \tilde{t}_L, \tilde{u}_R, \tilde{c}_R, \tilde{t}_R)^T, \quad (3)$$

$$(\tilde{d}_1, \dots, \tilde{d}_6)^T = R^d(\tilde{d}_L, \tilde{s}_L, \tilde{b}_L, \tilde{d}_R, \tilde{s}_R, \tilde{b}_R)^T. \quad (4)$$

By convention, the squark mass eigenstates are labelled according to  $m_{\tilde{q}_i} < \dots < m_{\tilde{q}_6}$  for  $q = u, d$ . All relevant couplings are then generalized by expressing them in terms of  $R^u$  and  $R^d$ .

## 2 Constraints on NMFV in mSUGRA

In order to take implicitly into account a number of experimental bounds coming from the neutral kaon sector,  $B$ - and  $D$ -meson oscillations, rare decays, and electric dipole moments [5, 6], we restrict ourselves to the case of flavour violation between only the second and third generations of left-chiral squarks, implemented through one real NMFV-parameter  $\lambda \equiv \lambda_{LL}^{sb} =$

$\lambda_{LL}^{ct}$ , while all other  $\lambda_{ij}^{qq'}$  are zero. Allowed regions for this parameter are then obtained by imposing explicitly low-energy, electroweak precision and cosmological constraints. We start with the theoretically robust inclusive branching ratio [7]

$$\text{BR}(b \rightarrow s\gamma) = (3.55 \pm 0.26) \times 10^{-4}, \quad (5)$$

which affects directly the allowed squark mixing between the second and third generation. Since NMFV contributes already at one-loop level, as do the SM contributions, this constraint is supposed to depend strongly on the NMFV-parameter  $\lambda$ . A second observable, sensitive to squark mass splitting and thus to NMFV, is the electroweak  $\rho$ -parameter, for which new physics contributions are constrained to [4]

$$\Delta\rho = -\alpha T = (1.02 \pm 0.86) \times 10^{-3}. \quad (6)$$

by the latest combined precision measurements. A third variable sensitive to SUSY loop corrections is the anomalous magnetic moment of the muon, for which we require the new physics contribution  $a_\mu^{\text{SUSY}}$  to close the gap

$$\Delta a_\mu = (22 \pm 10) \times 10^{-10} \quad (7)$$

between recent experimental data and the SM prediction [4]. Finally, to have a viable cold dark matter candidate, we require the lightest SUSY particle (LSP) to be neutral in electric charge and colour, and the resulting neutralino relic density  $\Omega_{\text{CDM}} h^2$  to agree with the observational limit [12]

$$0.094 < \Omega_{\text{CDM}} h^2 < 0.136. \quad (8)$$

The above limits are imposed at  $2\sigma$  confidence level on the mSUGRA model with five free parameters  $m_0$ ,  $m_{1/2}$ ,  $A_0$ ,  $\tan\beta$ , and  $\text{sgn}(\mu)$  at the GUT scale. The renormalization group equations are solved numerically to two-loop order using the computer programme SPheno 2.2.3 [13]. At the weak scale, we generalize the squark mass matrices by introducing the NMFV parameter  $\lambda$  as described above, diagonalize these matrices and compute the low-energy and electroweak precision constraints using the computer programme FeynHiggs 2.5.1 [14]. The neutralino relic density is computed using a NMFV-adapted version of the computer programme DarkSUSY 4.1 [11], taking into account the six-dimensional helicity and flavour squark mixing. For the Standard Model input parameters, i.e. the masses and widths of the electroweak gauge bosons and quarks, the elements of the CKM-matrix, the SM  $CP$ -violating phase, and Fermi's coupling constant, we refer the reader to Ref. [4].

The one-loop SUSY contributions to  $a_\mu^{\text{SUSY}}$  are proportional to  $\text{sgn}(\mu)$  [15], so that the disagreement between experiment and SM prediction is increased for  $\mu < 0$  in all SUSY models. As furthermore, this region is virtually excluded by the  $b \rightarrow s\gamma$  constraint for all  $\lambda \in [0; 0.1]$  except for very high SUSY masses, we restrict ourselves to the case of  $\mu > 0$ . The dependence on  $A_0$  of the variables is extremely weak, so that we use only  $A_0 = 0$  throughout our analysis.

**Table 1.** Benchmark points for mSUGRA allowing for flavour violation among the second and third generations. We also indicate the allowed range for the NMFV-parameter  $\lambda$ . The values of  $m_0$ ,  $m_{1/2}$  and  $A_0$  are given in GeV.

	$m_0$	$m_{1/2}$	$A_0$	$\tan\beta$	$\text{sgn}(\mu)$	$\lambda$ bounds
A	700	200	0	10	+	[0; 0.05]
B	100	400	0	10	+	[0; 0.10]
C	230	590	0	30	+	[0; 0.05]
D	600	700	0	50	+	[0; 0.05]

Fig. 1 shows a typical scan of the mSUGRA parameter space in  $m_0$  and  $m_{1/2}$  for  $\tan\beta = 10$ ,  $A_0=0$ , and  $\mu > 0$ , and different values of  $\lambda \in [0; 0.1]$ . As expected, the  $b \rightarrow s\gamma$  excluded region depends strongly on flavour mixing, while the regions favoured by  $a_\mu$  and the dark matter relic density show quite low sensitivity on the  $\lambda$ -parameter.  $\Delta\rho$  constrains the parameter space only for very high scalar ( $m_0 > 2000$  GeV) and gaugino ( $m_{1/2} > 1500$  GeV) masses, so that the corresponding regions are not shown.

Based on an extensive analysis of the mSUGRA parameter space at different values of  $\tan\beta$  (10, 30, and 50), we define benchmark scenarios, which are allowed/favoured by the above constraints, permit non-minimal flavour violation among left-chiral squarks of the second and third generation up to  $\lambda \leq 0.1$ , and are at the same time ‘‘collider-friendly’’, i.e. have relatively low values of  $m_0$  and  $m_{1/2}$ . Our choices are presented in Tab. 1, together with the corresponding allowed ranges for the NMFV-parameter  $\lambda$ . Note that all four benchmark points are also valid in MFV ( $\lambda \leq 0.005 \dots 0.01$ ) and cMFV ( $\lambda = 0$ ) scenarios.

### 3 Numerical discussion

In this talk, we focus on the phenomenology of benchmark scenario B. For this point all sparticle masses are below 1 TeV (see Fig. 3), which makes it the most ‘‘collider-friendly’’ among the four proposed scenarios, having light sleptons ( $m_{\tilde{l}} \sim 200 \dots 300$  GeV), relatively light gauginos ( $m_{\tilde{\chi}} \sim 150 \dots 550$  GeV) and squarks ( $m_{\tilde{q}} \sim 650 \dots 850$  GeV), as well as a heavy gluino ( $m_{\tilde{g}} \sim 900$  GeV). For a similar discussion of the other points presented in Tab. 1, the reader is referred to Ref. [16].

The explicitly imposed constraints are shown in Fig. 2, except for the SUSY contribution to the anomalous magnetic moment of the muon,  $a_\mu^{\text{SUSY}} \simeq 14 \times 10^{-10}$ , that is independent of  $\lambda$  and agrees with the limits in Eq. (7). The first graph shows the electroweak precision observable  $\Delta\rho$ . On our logarithmic scale, only the upper bound of the  $2\sigma$  range is visible. Despite the strong dependence of  $\Delta\rho$  on squark flavours, helicities and masses, the experimental error is sufficiently important to allow for relatively large values of  $\lambda \leq 0.52$ . The most stringent low-energy constraint comes from the  $b \rightarrow s\gamma$  branching ratio, which depends strongly

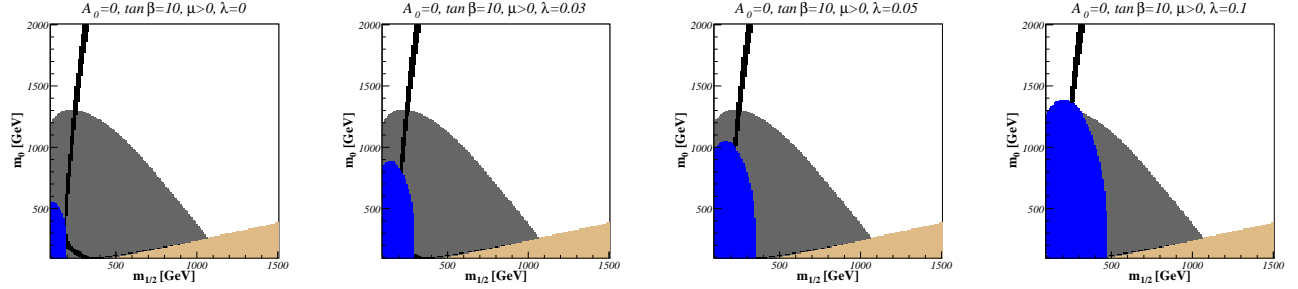


**Fig. 1.** The  $(m_0, m_{1/2})$ -planes for  $\tan \beta = 10$ ,  $A_0 = 0$ ,  $\mu > 0$ , and  $\lambda = 0, 0.03, 0.05, 0.1$ . We show  $a_\mu$  (grey) and WMAP (black) favoured as well as  $b \rightarrow s\gamma$  (blue) and charged LSP (beige) excluded regions of the mSUGRA parameter space in constrained minimal ( $\lambda = 0$ ) and non-minimal ( $\lambda > 0$ ) flavour violation.

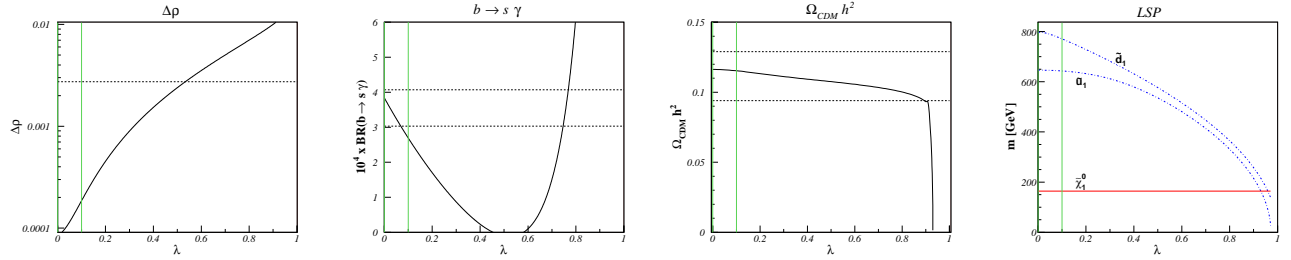


**Fig. 2.** Dependence of the precision variables  $\text{BR}(b \rightarrow s\gamma)$ ,  $\Delta\rho$ , and the cold dark matter relic density  $\Omega_{\text{CDM}}h^2$  as well as the lightest neutralino, up- and down-type squark masses on the NMFV-parameter  $\lambda$  in our benchmark scenario B. The experimentally allowed ranges (within  $2\sigma$ ) are indicated by horizontal dashed lines.

on the NMFV-parameter  $\lambda$  due to the same loop-level of the SUSY and SM contributions. The small experimental error allows for two narrow intervals in  $\lambda$ . As the second one is disfavoured by  $B \rightarrow X_s \mu^+ \mu^-$  [17], we restrict ourselves to the region  $\lambda \leq 0.1$ . The neutralino relic density  $\Omega_{\text{CDM}}h^2$  agrees with the limits in Eq. (8) up to high values of  $\lambda \leq 0.9$ , which is due to the fact that in the relevant neutralino (co)annihilation processes squarks only appear as propagators or at one-loop level. The decreasing of  $\Omega_{\text{CDM}}h^2$  for higher  $\lambda$  is due to the larger mass splitting of the squarks, implying that the lightest up- and down-type squarks become lighter and coannihilation processes become more important.

Fig. 3 shows the mass eigenvalues of the up- and down-type squarks as a function of the NMFV parameter  $\lambda \in [0; 0.1]$ . We observe large mass splitting for the lightest and heaviest squarks with increasing  $\lambda$  due to the growing relative importance of the off-diagonal matrix elements. However, the masses of the intermediate squarks are practically insensitive to  $\lambda$ . Another interesting phenomenon observed is the so-called “avoided crossing” between the squark mass eigenvalues. For the down-type squarks for example, this is observed at  $\lambda \approx 0.02$  between the states  $\tilde{d}_1$  and  $\tilde{d}_3$  (see Fig. 3). At the point where two levels should cross, the corresponding squark eigenstates mix and change character (see Fig. 4). The same phenomenon occurs also for the up-type squarks at  $\lambda \approx 0.02$  between  $\tilde{u}_4$  and  $\tilde{u}_5$ , and a second time at  $\lambda \approx 0.1$  between  $\tilde{u}_3$  and  $\tilde{u}_4$ . These “avoided crossings”, a common phenomenon in quantum mechanics, are due to the fact that the Hermitian squark mass matrix depends continuously on one single real parameter  $\lambda$ .

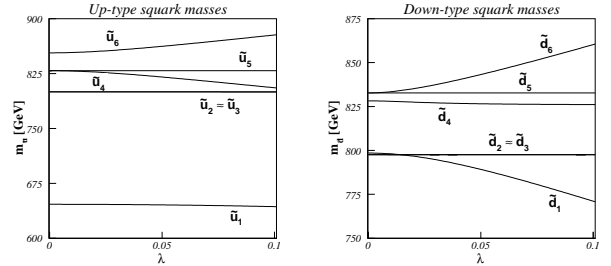


**Fig. 3.** Dependence of the up- and down-type squark masses on the NMFV-parameter  $\lambda$  in our benchmark scenario B.

In Fig. 4 we show the helicity and flavour decomposition of some of the up- and down-type left-handed squark mass eigenstates for the experimentally favoured range in the vicinity of (c)MFV, i.e.  $\lambda \in [0; 0.1]$ .

We finally provide numerical predictions for production cross sections of squarks and gauginos at the LHC, i.e. for  $pp$ -collisions at  $\sqrt{s} = 14$  TeV centre-of-momentum energy. Fig. 5 shows the numerical results for some interesting channels in our benchmark scenario B. Again, for a complete discussion of all channels in all four benchmark scenarios, the reader is referred to Ref. [16]. The magnitudes of the cross sections vary from barely visible level ( $10^{-2}$  fb) for weak production of heavy final states over the semi-strong production of squarks and gauginos and quark-gluon final states to large cross sections ( $10^2$  to  $10^3$  fb) for the strong production of diagonal squark-(anti)squark pairs or weak production of very light gaugino pairs. Unfortunately, since the strong gauge interaction is insensitive to (s)quark flavours and gaugino pair produc-

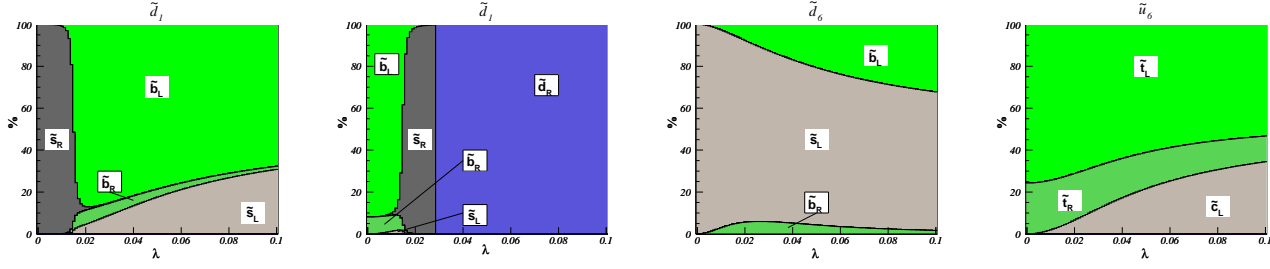


**Fig. 4.** Dependence of the chirality (L, R) and flavour ( $u$ ,  $c$ ,  $t$ ;  $d$ ,  $s$ , and  $b$ ) content of the discussed up- and down-type squark mass eigenstates on the NMFV-parameter  $\lambda \in [0; 0.1]$  for benchmark scenario B.

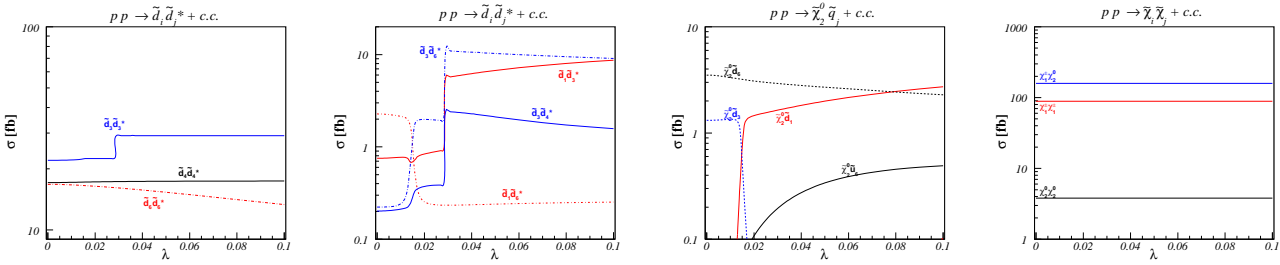


**Fig. 5.** Cross section examples for charged and neutral squark-antisquark pair, associated squark-neutralino, and gaugino-pair production at the LHC as function of the NMFV-parameter  $\lambda \in [0; 0.1]$  in our benchmark scenario B.

tion cross sections are summed over exchanged squark flavours, the processes with the largest cross sections are practically insensitive to the flavour violation parameter  $\lambda$ .

Some of the subleading, non-diagonal cross sections, however, show sharp transitions. For example, at  $\lambda = 0.02$ , the cross sections for  $\tilde{d}_1 \tilde{d}_6^*$  and  $\tilde{d}_3 \tilde{d}_6^*$  switch places, corresponding to an avoided crossing in the mass eigenvalues and a switch in the flavour contents of the  $\tilde{d}_1$  and  $\tilde{d}_3$  squarks (see Figs. 3 and 4). Since the concerned  $s$ -strange and  $s$ -bottom mass differences are rather small, this is mainly due to the different strange and bottom quark densities in the proton. At  $\lambda = 0.035$ , the cross sections for  $\tilde{d}_3 \tilde{d}_6^*$  and  $\tilde{d}_1 \tilde{d}_3^*$  increase sharply, corresponding to the flavour content change in the  $\tilde{d}_3$  squark from  $\tilde{s}_R$  to  $\tilde{d}_R$  (see Fig. 4), that can now be produced from down valence quarks. The  $\tilde{d}_1 \tilde{d}_3$  production cross section increases with the strange squark content of  $\tilde{d}_1$ .

Smooth transitions and semi-strong cross sections of about 1 fb are observed for the associated production of third-generation squarks with charginos and neutralinos. The cross section for  $\tilde{d}_6$  production decreases with its strange squark content, while the bottom squark content increases at the same time (see Fig. 4). The opposite happens for  $\tilde{d}_3$ , where the production cross section increases. For the up-type squarks, the cross section of  $\tilde{u}_6$  production increases/decreases with its charm/top squark content.

## 4 Conclusion

We have presented an implementation of NMFV in the MSSM at the weak scale. The relevant flavour violating off-diagonal elements of the squared squark

mass matrix are parametrized by one real NMFV parameter. Based on an extensive analysis of low-energy, electroweak precision and cosmological constraints, we proposed benchmark points for the mSUGRA scenario including NMFV. We discussed the phenomenology of these benchmark scenarios, which are characterized by the phenomenon of “avoided crossings”. We finally presented numerical predictions for squark and gaugino production cross sections at the LHC, among which several processes are sensitive to NMFV.

## References

1. J. F. Donoghue *et al.*, Phys. Lett. B **128** (1983) 55; M. J. Duncan, Nucl. Phys. B **221** (1983) 285; A. Bouquet *et al.*, Phys. Lett. B **148** (1984) 69; F. Borzumati *et al.*, Phys. Rev. Lett. **57** (1986) 961.
2. F. Gabbiani *et al.*, Nucl. Phys. B **322** (1989) 235.
3. F. Gabbiani *et al.*, Nucl. Phys. B **477** (1996) 321.
4. W. M. Yao *et al.*, J. Phys. G **33** (2006) 1.
5. M. Chiuchini *et al.*, hep-ph/0702144; J. Foster *et al.*, Phys. Lett. B **641** (2006) 452.
6. T. Hahn *et al.*, hep-ph/0512315.
7. E. Barbiero *et al.*, hep-ex/0603003.
8. A. L. Kagan *et al.*, Phys. Rev. D **58** (1998) 094012.
9. S. Heinemeyer *et al.*, Eur. Phys. J. C **37** (2004) 481.
10. S. Heinemeyer *et al.*, Nucl. Phys. B **690** (2004) 62; S. Heinemeyer *et al.*, Nucl. Phys. B **699** (2004) 103.
11. P. Gondolo *et al.*, JCAP **0407** (2004) 008.
12. J. Hamann *et al.*, Phys. Rev. D **75** (2007) 023522.
13. W. Porod, Comput. Phys. Commun. **153** (2003) 275.
14. S. Heinemeyer *et al.*, Comput. Phys. Commun. **124** (2000) 76.
15. T. Moroi, Phys. Rev. D **53** (1996) 6565; T. Moroi, Phys. Rev. D **56** (1997) 4424 Erratum.
16. G. Bozzi *et al.*, Nucl. Phys. B (2007) in press, arXiv:0704.1826 [hep-ph].
17. P. Gambino *et al.*, Phys. Rev. Lett. **94** (2005) 061803.